Fabrication of cellulase catalysts immobilized on a nanoscale hybrid polyaniline/cationic hydrogel support for highly efficient catalytic conversion of cellulose

Afsaneh Zarei[a], Farzaneh Alihosseini*[a], Dambarudhar Parida[b], Rashid Nazir[b], Sabyasachi Gaan[b]

[a] Department of Textile Engineering, Isfahan University of Technology, Isfahan, 84156-83111, Iran

[b] Laboratory of Advanced Fibers, Empa, Swiss Federal Laboratories for Materials Science and Technology, Lerchenfeldstrasse 5, CH-9014 St. Gallen, Switzerland

* Corresponding author. E-mail: fhosseini@cc.iut.ac.ir, (Farzaneh Alihosseini, Fax: (+98) 31 339115014)

Abstract. A novel conductive nano-hydrogel hybrid support was prepared by in-situ polymerization of polyaniline nanorods on an electrospun cationic hydrogel of poly (ε-caprolactone) (PCL) and a cationic phosphine oxide macromolecule. Subsequently, the cellulase enzyme was immobilized on the hybrid support. Field emission scanning electron microscope (SEM) and Brunauer–Emmett–Teller (BET) analyzes confirmed mesoporous, rod-like structures with slit-like pore geometry for the immobilized support and exhibiting a high immobilization capacity and reduced diffusion resistance of the substrate. For comparison, the catalytic activity, storage stability and reusability of the immobilized and free enzyme were evaluated. The results showed that the immobilized enzymes have higher thermal stability without change in the optimal pH (5.5) and temperature (55 °C) for enzyme activity. A high immobilization efficiency (96 %) was observed for the immobilized cellulose catalysts after optimization of parameters such as pH, temperature, incubation time and protein concentration. The immobilized enzyme retained almost 90% of its original activity after four weeks of storage and 73% of its original activity after the 9th reuse cycle. These results strongly suggest that the prepared hybrid support has the potential to be used as a support for protein immobilization.

Keywords: nano hydrogel; polyaniline; cellulase; immobilization, electrospinning

1. Introduction.

Enzyme immobilization on a variety of insoluble polymers and inorganic materials[1–3] is one of the most attractive topics in enzyme technology. There are many reports on the effectiveness of enzyme immobilization not only in improving enzyme stability but also in enhancing recyclability[4–7].

Reports on the application of different immobilization strategies including covalent immobilization on magnetic poly(ionic liquid)[8], adsorption on anchored polyacrylonitrile film[9], physical adsorption on multiwall carbon nanotubes[10] and so on illustrated improved features for the target immobilized enzyme. Among various support materials, hydrogels due to the ability to simulation the microenvironment of a free enzyme[11] have the potential to be the leading carrier for keeping the biomolecule active and stable. However, the fairly weak interaction with the target molecule is one of their limitation[12]. To overcome this drawback, many researchers have investigated the effect of surface modifying functional groups[6,13].

The use of conducting polymers such as polyaniline (PANI) either as biomolecule carriers[14] or surface modifiers[9,15] is extensively investigated. PANI is a relatively low-cost polymer, has ease of synthesis and good stability to extreme temperatures and pH, and is also resistant to microbial attack[16,17]. The presence of electrically conductive materials such as PANI in hydrogels has contributed to the development of multifunctional smart hydrogels that combine the mechanical and swelling properties of hydrogels with the specific characteristic of conductive polymers[18,19]. The use of polystyrene-divinylbenzene microspheres coated with PANI[15], polyaniline nanofibers[20] and self-cross-linked PANI hydrogel[21] showed enhanced properties for immobilization of cellulase by adsorption and adsorption/crosslinking methods, electromagnetic shielding properties and electrochemical energy storage, respectively.

Cellulase is the third most widely used industrial enzyme with great potential for many commercial applications such as food, textile, biofuel and paper industries[22]. There are a lot of researches on using different support materials for cellulase immobilization. However, many of them have several drawbacks such as low loading capacity[15] and low reusability[23] because of the weak stability of the immobilized enzyme.

In a recent study[24,25] a cationic hydrogel was prepared via Michael addition reaction of tivinylphosphine oxide (TVPO) and piperazine under ambient conditions. In addition to the existing reports[26] on the effects of phosphine-containing polymers on controlling the size and shape of polymers, the synthesized gel showed other excellent properties, including response to external stimuli (pH, ionic strength, chemicals, and their combinations), easy penetration of water-soluble chemicals, and effective retention of biomolecule activity. More importantly, due to the cationic nature of the hydrogel and the possibility of electrostatic interactions, we investigated the potential application of this support for the immobilization of an acidic enzyme (cellulase with a low isoelectric point, pI=4.5) to overcome enzyme leaching from the hydrogel. Therefore, in the present work, considering the great advantages of nanofiber matrixes such as a high surface area to volume ratio, easy material combination, relatively low cost and more important the compatibility of the cationic hydrogel with the electrospinning process, a nanofiber hydrogel was fabricated through this method using in situ gelation technique as a first step. Taking advantage of the unique properties of PANI[27], PANI polymerization was then carried out on the prepared hybrid nano-hydrogel. PANI reduces enzyme leakage from the porous matrix through electrostatic interactions between the positive charge of the hybrid support and the net negative charge of the enzyme. Protein immobilization was thus preceded by a combination of adsorption and entrapment processes. The morphology, porosity and functional groups of the hybrid support were studied by field emission scanning electron microscope (FE-SEM), Brunauer–Emmett–Teller (BET) and Fourier transform infrared spectroscopy (FT-IR). The optimal immobilization conditions including temperature, pH, incubation time and protein concentration were determined. The reusability and storage stability of the immobilized cellulase were also evaluated. Meanwhile, the enzyme absorption capacity of PCL-Hydrogel-PANI, PCL-Hydrogel, and PCL was also investigated.

2. Experimental

2.1. Materials

Cellulase from *Trichoderma reesei* (Cat. No C2730, ≥700 U/g), bovine serum albumin (BSA), coomassie brilliant blue G-250, Whatman filter paper (Cat. No. 1001110), carboxymethyl cellulose (CMC), potassium sodium tartrate tetrahydrate, glucose, 3,5-dinitrosalicylic acid (DNS), aniline hydrochloride (99%, M_w=129.59 g/mol) and ammonium peroxydisulfate (APS, 98%, M_w =288.18 g/mol**),** were purchased from Merck AG (Germany). Poly(ε-caprolactone) (PCL, M_n=80000) and piperazine were obtained from Sigma Aldrich (United Kingdom). TVPO was synthesized according to a published work[24]. Analytical grade phosphoric acid, ethanol, methanol, hydrochloric acid, acetone, chloroform, and dimethylformamide (DMF) were purchased from Merck (Germany).

2.2. Preparation of hybrid support

2.2.1. Preparation of the electrospun PCL nano hydrogel (PHG)

To prepare uniform nanofibers, the PCL was dissolved in a mixed solvent containing chloroform and DMF with a ratio of 90:10 at a concentration of 8% w/v and stirred at ambient temperature for 24 hours. Subsequently, four different amounts of piperazine and TVPO (10, 25, 50, and 75%) in a 1:1 molar ratio mix (monomers of hydrogel) were added to the 8% w/v PCL solution, based on the previous study[24]. and stirred for 3h at room temperature to form a homogeneous solution. The well-mixed solution was pumped through the electro-spinning machine using a syringe pump. The end of the needle was connected to a high voltage DC power supply of 7 kV. The polymer solution was pumped at a rate of 0.18 ml/h and the distance from the tip of the needle to the collector was fixed at 12 cm based on preliminary results. The web of electrospun nanofibers was collected on a rotating collector which was wrapped with an aluminum foil after a run time of 3h. Then, the prepared electrospun mat was incubated for 4h at 40 °C to obtain a crosslinked network of TVPO and piperazine, which act as

the nano hydrogel (PHG). Table S.1 summarizes the composition of different electrospun samples prepared in this work.

2.2.2. Synthesis of PANI on the surface of PHG

In situ polymerization of polyaniline was carried out by the aniline hydrochloride monomers using APS as an oxidizing agent. A 0.2 M solution of aniline hydrochloride was prepared by dissolving the monomer in HCL 1M. Then the PHG web, as well as hydrogel (HG) (prepared based on the previous study[24]) were immersed in an aniline hydrochloride solution for 6h. To improve reaction yield the stoichiometric molar ratio of 1.25 of ammonium peroxydisulfate: monomer was selected. Polymerization was performed by the dropwise addition of APS to the already prepared monomer solution containing the PHG and HG under continuous shaking (130 rpm) at 5 °C for 30 min. In-situ polymerization was allowed for 6 h at 5 °C to complete the polymerization.

The green PANI coated PHG web (PHG.PN) and HG (HG.PN) were removed and washed several times by acetone and deionized water, respectively, and dried at room temperature. Pure PANI was also synthesized by this method for comparison. The electrospun web was weighed before and after this treatment.

The amount of polymer loaded on the surface of the PHG web was calculated by the gravimetric method according to the following Eq.1:

$$Loading\ percentage\ (\%) = \left(\left(M_p - M_w\right)/M_w\right) \times 100 \quad (1)$$

Where M_w and M_p are the weight of nano hydrogel web before and after polymerization of aniline hydrochloride, respectively.

2.3. Enzyme immobilization

Firstly, different starting amounts of the protein (1, 5, 10, 20, 30, 50, 70, 100 mg/ml) were dissolved at various pH in acetate buffer (5 ml, 50mM, pH 3.5-7.5). Then, 5mg of each PCLweb, PHG75 web, and PHG75.PN (PANI coated nanoweb with 75% hydrogel) was immersed in the prepared enzyme solution at a certain temperature (25-75℃) and continuous shaking of 130 rpm was carried out for a specific time (1-4 hour). After the immobilization process, the sample was removed from the enzyme solution and washed three times with the same fresh buffer solution to separate the loosely attached enzyme and dried at room temperature overnight. The washing solutions were kept to determine the exact amount of immobilized cellulase. The enzyme immobilized samples were preserved at 4°C before each study.

2.4. Effect of pH and temperature on free and immobilized enzyme

To evaluate the effect of pH on the enzyme activity, the optimized sample was used for the hydrolysis of the Whatman filter paper in 5 ml of acetate buffer 50mM, pH range 3.5-7.5 at 45 ℃. The effect of temperature on the activity of the enzyme was also assayed in the temperature range 25-75℃, in 5 ml of acetate buffer 50mM at pH 5.5. The thermal stability of the immobilized enzyme was also investigated at 75℃, in 5 ml of acetate buffer 50mM at pH 5.5 for 180 min.

The enzyme activity recovery was calculated using observed activity (μmol. min^{-1}) compared to that of the total starting activity of the free enzyme (μmol. min^{-1}) by the following Eq.2[28]:

$$Activity\ recovery\ (\%) = (observed\ activity/starting\ activity) \times 100 \quad (2)$$

2.5. The Bradford method for determination of enzyme loading efficiency

protein concentration was measured by the Lowry method using bovine serum albumin (BSA) as the standard[29]. The assay reagent was made by dissolving 10 mg coomassie brilliant blue G-250 in 5 ml of 95% ethanol. The solution was then mixed with 10 mL of 85% phosphoric acid and made up to 100 ml with distilled water. BSA was used as a stock solution for the calibration curve. To plot the

calibration curve, different concentrations of BSA were utilized, and the absorbance of these solutions was measured at 595 nm after adding Bradford's reagent, using a UV-VIS spectrophotometer (Shimadzu UVmini-1240, Japan). The enzyme loading per unit weight of hybrid support (wt%) after washing, immobilization yield and immobilization efficiency was calculated as following Eqs. 3, 4, and 5, respectively[28].

$$protein\ loading(wt\%) = (((M_0 - M_t)V_s - (M_w \times V_w))/W) \times 100 \quad (3)$$

$$Yield(\%) = (immobilized\ activity/starting\ activity) \times 100 \quad (4)$$

$$Efficiency(\%) = (observed\ activity/immobilized\ activity) \times 100 \quad (5)$$

In equation. 3, M_0, M_t, and M_w are the initial protein concentration, the amount of enzyme in the solution after time t, and the enzyme concentration in the wash solution (mg/ml), respectively. V_s and V_w are the volume of enzyme solution and wash solution (ml), respectively. W is the weight of PHG75.PN (mg). All the activity terms were calculated by using the total activity (μmol. min^{-1}).

2.6. Measurement of the free and immobilized enzyme activities

The total hydrolytic activity of free and immobilized cellulase was measured based on the DNS method after enzymatic hydrolysis of the Whatman filter paper as the substrate. 100 ml assay mixture was prepared by dissolving 1.6 g NaOH, 1 g DNS, and 25 g sodium-potassium tartrate in distilled water. An appropriate amount of assayed sample and 3 ml DNS solution were mixed and then boil for exactly 15 min in a boiling water bath containing sufficient water. After transfer to a cold-water bath, the intensity of the color formed was measured at 540 nm[30]. To measure the amount of reducing sugar formed after hydrolysis in the unknown solution, a standard curve of glucose was plotted by different concentrations of glucose solution.

One unit (U) of the enzyme is defined as the amount of enzyme that catalyzes the reaction of 1 μmol of substrate per unit of time (one minute) under standard conditions. The cellulase activity was

determined by using Eq.6. Where A is the amount of glucose produced after enzymatic hydrolysis (mg), M is the molecular weight of glucose (g/mol), V is the volume of the measured solution (ml) and t is the reaction time (min).

$$cellulase\ activity(\mu mol.ml^{-1}.min^{-1}) = (1000A)/(MVt) \quad (6)$$

2.7. Storage stability of the free and immobilized enzyme

The storage stability of the free and immobilized enzyme incubated at 4 ℃ was determined in an acetate buffer (50mM, pH5.5) after 4 weeks by calculating the residual activity. The residual activity is defined as the fraction of hydrolytic activity after immobilization on the hybrid support compared to the initial activity.

2.8. Reusability of immobilized enzyme

To measure the effectiveness of the immobilization reusability study was carried out using an insoluble substrate such as filter paper and a soluble substrate like CMC. In both cases, 5 mg PHG75.PN containing 49.08 mg of the enzyme was immersed in 5 ml water (at pH5.5 and 55 °C) containing 1% w/v of CMC or Whatman filter paper (50mg, 1×6 cm) at 55℃. After one hour, the enzyme immobilized sample was removed and washed three times with water (at pH5.5) before immersing it into a fresh reaction mixture for the next cycle. After that, each reaction mixture was centrifuged (25000 rpm, 5 min) to determine the amount of glucose produced as described in section 2.6.above.

2.9. Evaluation of kinetic constants of free and immobilized enzyme

The maximum rate of hydrolysis substrate (V_{max}) and $K_m$were assayed by Lineweaver-Burk plot for free and immobilized enzyme. The rate of the hydrolysis reaction for both free and immobilized enzymes was assayed by measuring the glucose concentration as a function of time for four amounts of CMC (0.5-2.5% w/v) in acetate buffer pH 5.5, 50mM. The initial rate of product formation in each CMC concentration was determined by the slope of the linear fit of the data of glucose concentration

vs. time. Then the V_{max}(mg. ml^{-1}.min^{-1}) and K_m (mg. ml^{-1}) were obtained by measuring the intercept and intersection with the x-axis of the Lineweaver-Burk plot based on Eq.7. Where, *V* is the initial rate (mg. ml^{-1}.min^{-1}) and [S] is equal to the substrate concentration (mg. ml^{-1}).

$$V = (V_{max}\,[S])/(K_m + [S]\,) \tag{7}$$

2.10. Characterization of the hybrid support

Field Emission scanning electron microscopy (FE-SEM (XL-30), Philips, Netherlands) was used to evaluate the morphology of developed hybrid support. The mean fiber diameter and distribution were obtained by measuring 100 fibers at different locations. Then, a Fourier-transform infrared spectrometer (BOMEM FT-IR MB-series, Hartmann & Braun, Canada) was used to characterize the functional groups of different samples. Before FT-IR analysis, the nanoweb sample and KBr were mixed uniformly and pressed to form a tablet.

The surface area and the pore size distribution were also determined by Brunauer–Emmet–Teller (BET) and Barret–Joyner–Halender (BJH) methods. The adsorption isotherms were obtained at a relative pressure (P/P_0) up to ~0.95 at 77K. To ensure the accuracy of the N_2 adsorption/desorption experiment, samples were dried under reduced pressure at 40 °C for 24h.

To determine the swelling ratio (SW%) of nanofiber samples, the known weight of dried nanofiber web (W_0) was immersed in30 ml of water in a beaker (at pH 5.5 and 25℃) and kept for a known duration. Then, the sample was carefully removed from the water and lightly wiped with wet filter paper to remove excess water and weighed (W_t). The percentage of swelling% was determined using Equation 8.

$$SW(\%) = ((W_t - W_0)/W_0) \times 100 \tag{8}$$

3. Results and Discussion

3.1. Synthesizing of the PANI coated hydrogel nano-web

Electro-spinning is a highly desirable method to produce high surface area and long-term durable nanostructures. The simplicity of the manufacturing process and the ability to control fiber diameter make this technique extremely attractive to develop solid supports. As hydrogel formed by mixing two monomers does not have a specific shape[24], electrospun PCL was used as a scaffold to generate the nanofibers with the high specific surface area in this study. To select the appropriate concentration of PCL for electro-spinning, the 7, 8, and 9% w/v of PCL solutions were prepared. The preliminary observation with optical microscopy (Fig. S2) showed that nanofibers from 8% w/v PCL solution achieved uniform and beadless morphology, while 7% and 9% were unable to form continuous filaments and some beads were observed inside the nanofibers. Thus, this concentration of PCL was chosen to develop hydrogel-based solid support. To do so, different concentrations (10, 25, 50, and 75% w/w) of piperazine and TVPO in a 1:1 molar ratio was added to 8% w/v PCL solution, and nanofiber was prepared through electrospinning by adjusting different electrospinning parameters including the needle-collector distance, flow rate, and applied voltage.

In the next step, nanofibrous-web containing 10, 25, 50, and 75 wt% of hydrogel were exposed to the PANI polymerization. Photographs of PHG75 nano-web before and after in-situ oxidative polymerization of PANI are shown in Fig. S1. Although the pristine PHG75 was white, after the growth of the polyaniline, the color has changed to green. This observation revealed that the coating of the PANI had been extended over the whole PHG75 sample. The PANI polymerization was further confirmed by FT-IR and FE-SEM images of the coated (PHG75.PN) and uncoated PHG75.

The FE-SEM images of PANI coating nano-webs with different percentages of the hydrogel are shown in Fig. 1. Considering the value of PANI coating percentage on hydrogel and PCL nano-webs, it was found that a combination of PCL and hydrogel as well as increasing the percentage of the cationic hydrogel from 10 to 75% led to the enhancement of PANI coating on the surface of nanofibers from 33% for PCL nanoweb to 76% for PHG.75. High penetration and absorption of aniline monomer into

the gel could be attributed to the cationic absorption capacity of hydrogel that was confirmed earlier[24], followed by a possible reaction between active groups of hydrogel and aniline monomers which will be discussed later in the FT-IR analysis section. It was noticeable from the FE-SEM result (Fig. 1) that despite the increased amount of PANI synthesized on hydrogel nano-webs, the pristine PCL nano-web did not show a significant amount of coating, emphasizing the vital role of the hydrogel in nano-webs in this regard.

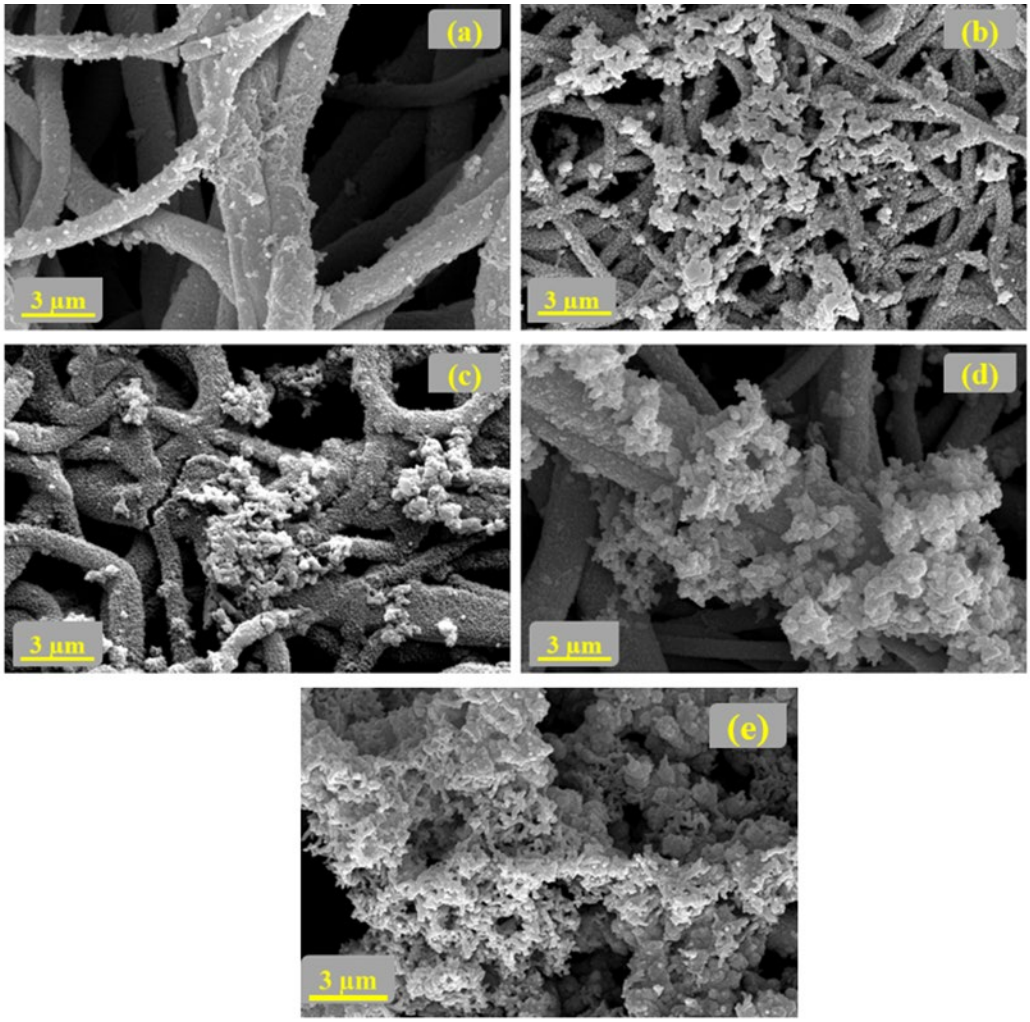

Fig. 1. FE-SEM images of PANI coated (a) PCL nano-web (PCL-PANI), (b) nanofibrous-web containing 10 wt% hydrogel (PHG10), (c) nanofibrous-web containing 25 wt% hydrogel PHG25, (d)

nanofibrous-web containing 50 wt% hydrogel PHG50 and (e) nanofibrous-web containing 75 wt% hydrogel PHG75.

The FE-SEM images of PCL, PHG75, and PHG75.PN are shown in Fig. 2. With the increased content of hydrogel in the support, not only the amount of PANI deposited has increased, but also some irregular polyaniline nanorods of approximately 98±20nm in diameter were observed on the surface of the nano-web. This result was important because some other researchers have also pointed out that the prepration of polyaniline nanostructures (diameter ≤100 nm) usually requires very specific and bulky dopants or relies on the use of templates (hard/soft templates) that require post-synthetic steps for elimination[18,20,21].

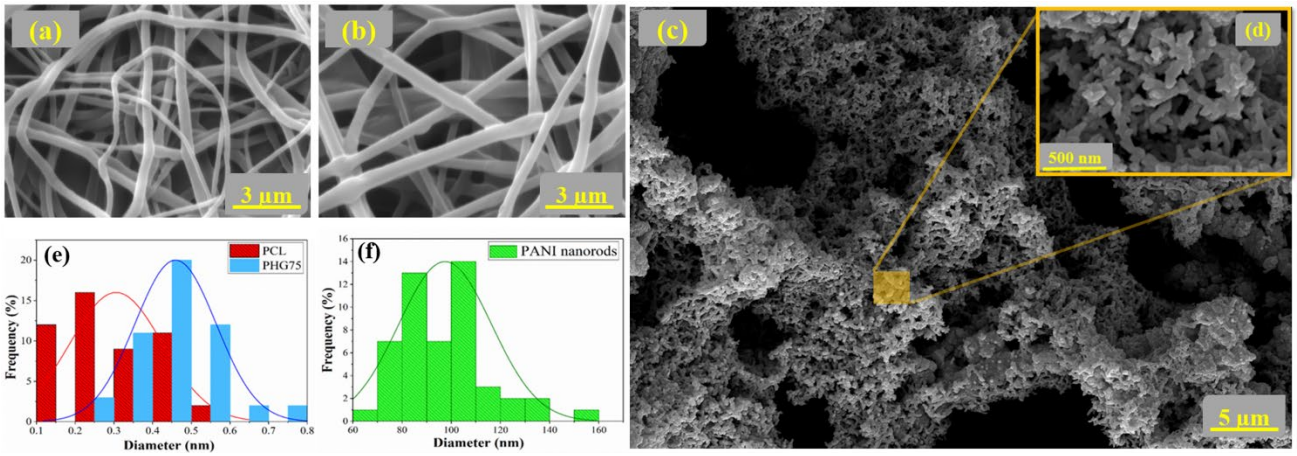

Fig. 2. FE-SEM images of (a) pristine PCL nanofibers, (b) nanofibers formed by a combination of PCL and 75 wt% hydrogel (PHG75), (c,d) PANI coated PHG75 nano-web(PHG75.PN) with different resolutions. (e,f) Diameter distribution of PCL, PHG75, and PANI nanorods, respectively.

3.2. FT-IR analysis

To confirm the successful reaction between monomer units and the formation of the hydrogel in the final nanofibrous structure, FT-IR analysis was done. The FT-IR spectra of the pure TVPO, piperazine, hydrogel, and PCL were also measured for comparison (Fig. S3). Analysis of TVPO spectra revealed

four characteristic peaks at 1600, 3082, 1956, and 1170 cm^{-1} corresponding to the C=C double bond, C-H bond of the vinyl group, an overtone of $C=CH_2$ and P=O stretching vibration[31], respectively. Piperazine had principal peaks in the regions around 1269 and 3236 cm^{-1} related to the C-N and N-H stretching vibrations of secondary aliphatic amine[32]. As exhibited in Fig. 3a, the formation of the tertiary amine is arising from the reaction between unsaturated carbon of TVPO (C=C) and NH groups of piperazine leads to the generation of the hydrogel (HG). The appearance of a peak at 1000 cm^{-1} related to the newly formed aliphatic tertiary amine[20] and the elimination of the N-H group (peak at1570 in piperazine spectrum) in PHG75 and HG illustrate the formation of the hydrogel (Fig. S3). The presence of a peak around 1658 cm^{-1} in the HG and PHG75 spectra can correspond to the unreacted vinyl groups of the TVPO.

A comparison of the IR spectral bands of the pure TVPO and HG indicates the absorption frequency of P=O is shifted from 1170 to 1145 cm^{-1}. It is assumed that the existence of nitrogen atoms as donor groups induce a negligible amount of electron to the system and that is responsible for shifting the vibrational frequency to a lower wavenumber. However, no such shift occurred in the PHG75 spectra. It can be related to the overlapping of the P=O peak with the C-O vibration peak attributed to the PCL. Besides, the C=O band of the carbonyl group in PCL is observed at 1724 cm^{-1}(Fig. S3).

The functional groups of PANI within the PHG75.PN was also identified by its typical peaks in the FT-IR spectra (Fig. S4). The characteristic peak at 800 cm^{-1} corresponds to the out-of-plane C-H bending which illustrates the formation of emeraldine salt of polyaniline. The band observed at 1236 cm^{-1} and the broadband at 1140 cm^{-1}, which are overlapped with P=O of TVPO, are attributed to π electron delocalization and exhibit high electron conductivity[19,33]. The absorbance peaks located at 1475 and 1563 cm^{-1} were assigned as the C=C stretching vibration of benzenoid (B-NH-B) and quinoid (Q=N=Q) rings, respectively[32]. The band at 1300 cm^{-1} originated from the C-N of secondary aromatic amine stretching of PANI. More interestingly, the peak at 1658 cm^{-1} related to the C=C of

unreacted vinyl groups of TVPO is decreased in PHG75.PN (Fig. 3b). This result might be due to the reaction between aniline hydrochloride and the terminal vinyl groups. The creation of PANI nanorod morphology may be explained by nucleation and precipitation theory[34], where, aniline hydrochloride reacts with the terminal vinyl and amino group of the hydrogel (Fig. 3c). This is confirmed by the disappearance of the FT-IR peak corresponding to residual vinyl groups (1658 cm^{-1}) in PHG75.PN (Fig. 3a) as well as HG.PN (Fig. S5). A similar observation has been reported in the literature to produce star-shaped PCL-PANI[35]. Since the oxidation of the growing polymer chain is more desirable than a monomer[36], the aniline monomers prefer to react with the existing growing polymer chains rather than at the support surface and leading to the generation of PANI nanorods.

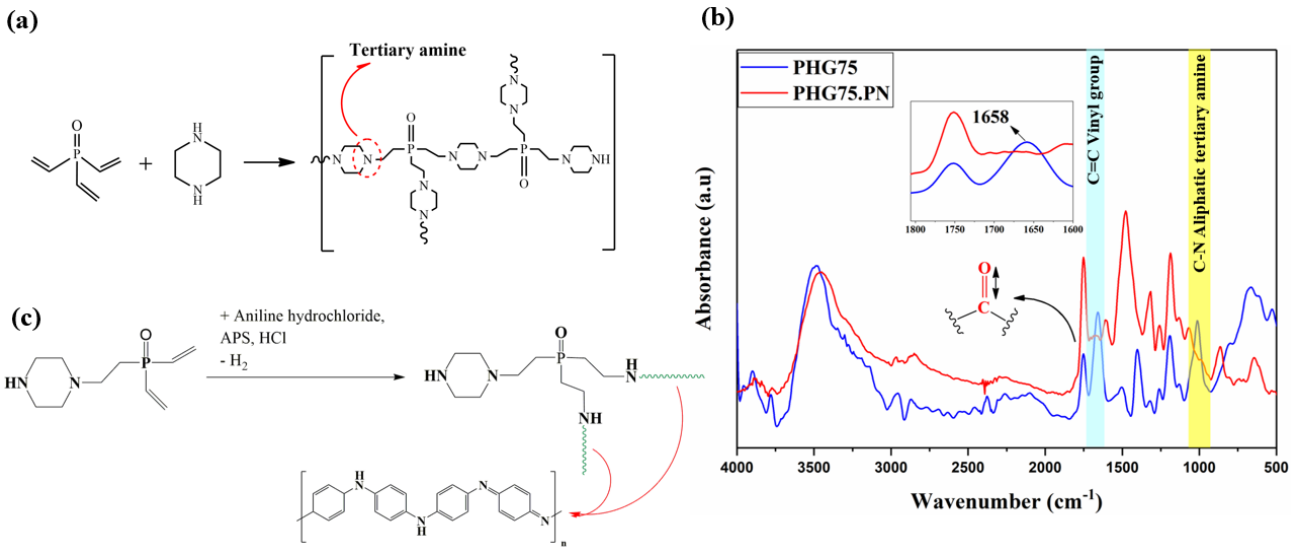

Fig. 3. (a) Schematic representation of phosphine oxide cationic hydrogel formation from TVPO and piperazine, (b) FT-IR spectra of PHG75 and PHG75.PN and (c) the possible reaction between unsaturated vinyl groups of hydrogel and polyaniline monomers.

Additionally, as seen in Fig.1c, d, the formation of the three-dimensional nanofibrous structure has created a larger surface area. So the BJH analysis was further used to examine the pore size distribution of the PANI coated support.

3.1.2. BET specific surface area and pore size distribution analysis

To study the effect of PANI nanorod formation on the adsorption efficiency of the produced hybrid support, the PHG75, and PHG75.PN was analyzed using Nitrogen adsorption/desorption isotherms. N_2 adsorption/desorption isotherms of PHG75.PN (Fig. 4a) was exhibited type-IV isotherm with a type-H3 hysteresis according to the IUPAC classification, indicating a mesoporous structure with slit pore geometry. The N2 adsorption/desorption isotherms of PHG75, as a control hydrogel nanofiber before PANI polymerization, were performed and the results in (Figure S6a) show that it is a microporous solid as it forms a type-I isotherm. For complete characterization, the pore size distribution of PHG75.PN and PHG75 from the desorption branch were determined by the BJH method (Figure 4b and Figure S6b). It was found that mesopores with a radius between 2 and 100 nm are present in PHG75.PN. Thus, PHG75.PN consists of a micropore base of PHG75 and a mesopore surface related to PANI nanorods[37]. N_2 physisorption experiments indicated an increase in the surface area from 20.2 m^2g^{-1} to 31.3 m^2g^{-1} and the pore volume from 0.007 cm^3g^{-1} to 0.06 cm^3g^{-1} for PHG75 and PHG75.PN, respectively, upon the PANI polymerization. It was obvious that the BET surface area of PHG75.PN was about 1.55 times higher than PHG75.

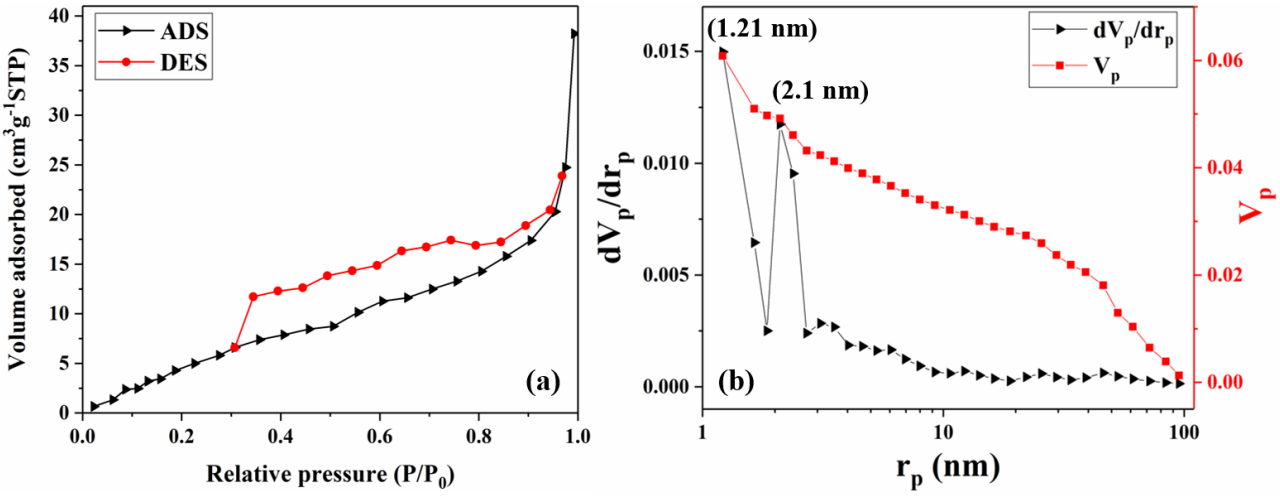

Fig. 4. (a) N_2 adsorption/desorption isotherms obtained at 77k (b) pore size distribution and pore volume of PHG75.PN.

3.2. Immobilization of enzyme onto the prepared hybrid support

3.2.1. Effect of pH, initial protein concentration, and incubation time on the immobilization efficiency.

As the immobilization conditions have a great influence on the loading efficiency and activity of the enzymes, the effects of pH, protein concentration, and incubation time were individually investigated. As shown in Fig. 5a, the highest immobilization efficiency and yield (~95% and ~90%, respectively) was achieved at pH 5.5. The isoelectric point (pI) of the enzyme is 4.5 and the maximum enzyme loaded on the matrix was observed at the point higher than its pI. At this pH, the average charge of the enzyme is negative, so there was an electrostatic interaction between the positive charges of the hybrid support arising from the protonation of PANI and the phosphine oxide macromolecules. In addition, physical entrapment, hydrophobic forces, hydrogen bonds, and van der Waals interaction could also contribute to the enzyme immobilization at pH 5.5[38].

The protein immobilization efficiency at different initial concentrations of 1-100 mg/ml at pH 5.5 and 45℃ is shown in Fig. 5b. It can be seen that by increasing the protein concentration from 1 to 50 mg/ml, the immobilization efficiency increased from 71% to 85% then decreased to 78% at 100 mg/ml. Although the higher immobilization yield (~85%) at lower enzyme concentrations means that a larger amount of enzyme was immobilized. The lowest activity was observed at the lowest immobilization efficiency. This could be related to the inaccessibility of the insoluble substrate to the active site of the enzyme immobilized in the fibrous structure of the support. On the other hand, the decrease in immobilization efficiency and yield at higher concentrations (70 and 100 mg/ml) may be due to the physical restrictions resulting from the steric hindrance of the enzyme molecules and saturation of the support.

A comparison between the amount of loaded protein (50 mg/ml) in this work with some reports on using different support materials such as magnetic nanoparticles[5], functionalized multiwall carbon nanotubes[10] or polyaniline coated microspheres[15] with 18, 4 and 3 mg/ml enzyme capacity, respectively, shows the high capacity of the designed support for biocatalyst immobilization. An excessive amount of enzymes would lead to layer-by-layer adsorption of enzyme molecules and either bury or block their active site, however, the hybrid support not only showed high protein capacity but also had high efficiency in this protein concentration. Hence, the 50 mg/ml enzyme solution was used in the following experiments. The FE-SEM image of the PHg75.PN after immobilizing of 50 mg/ml cellulase in Fig. 5c confirms uniform deposition of the enzyme on the hybrid support.

The incubation time of immobilization was checked from 1 to 4 hours and as shown in Fig. S7 the immobilization efficiency slightly increased to 95% after 3h. However, there was no significant difference between the immobilization efficiency after 1 and 3h of incubation time. Therefore, the rest of the experiments were carried out at the incubation time of 1h.

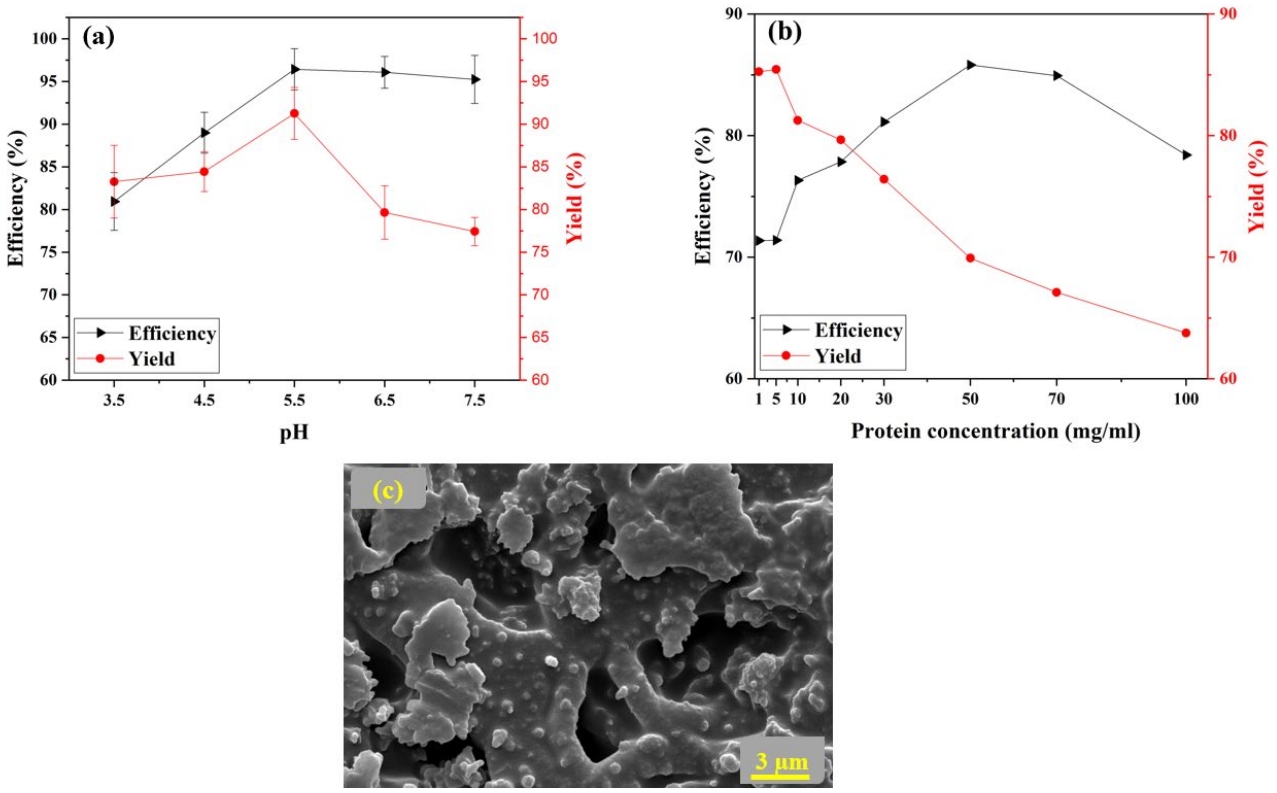

Fig. 5. (a) Effect of pH on the immobilization efficiency and yield of the enzyme, (b) Effect of the protein concentration on the immobilization efficiency and yield (c) FE-SEM image of PHG75.PN after protein immobilization.

3.2.2. The effect of polyaniline on the immobilization efficiency

To study the effect of PANI on the immobilization capacity of the hybrid support, the electrospun web of PCL and PHG75 were used for the immobilization of the enzyme under similar operating parameters (50 mg/ml cellulase solution, pH5.5, 1h, and 45℃). The results in Fig. 6a showed that the amount of immobilized enzyme increased from 13.5, 25.3, and 33.1 wt% For PCL, PHG75, and PHG75.PN, respectively. As already mentioned, the prepared hydrogel contains tertiary amine groups. At low pH, the tertiary amines are protonated resulting in the creation of positive charges in the network. So, the electrostatic repulsions between positively charged groups result in the swelling of the PHG75. More interestingly, the polyaniline chains also protonate in acidic pH, so a greater swelling behavior is

exhibited by PHG75.PN arises from two reasons, the existence of electrostatic repulsions in the backbone network and PANI chains and increasing hydrophilicity of PANI in its ionization state[39]. Fig. 6b illustrates the maximum swelling percentage of PCL, PHG75, and PHG75.PN were about 203.01%, 470%, and 572.33% after 6 h, respectively. The higher enzyme loaded in the PHG75.PN could be ascribed to the pore space between the PANI nanorods and its higher specific surface area besides its higher swelling ratio. The more loading efficiency of PHG75 compared to that of PCL was also related to the swelling ratio of the hydrogel in the aqueous medium during the protein immobilization process.

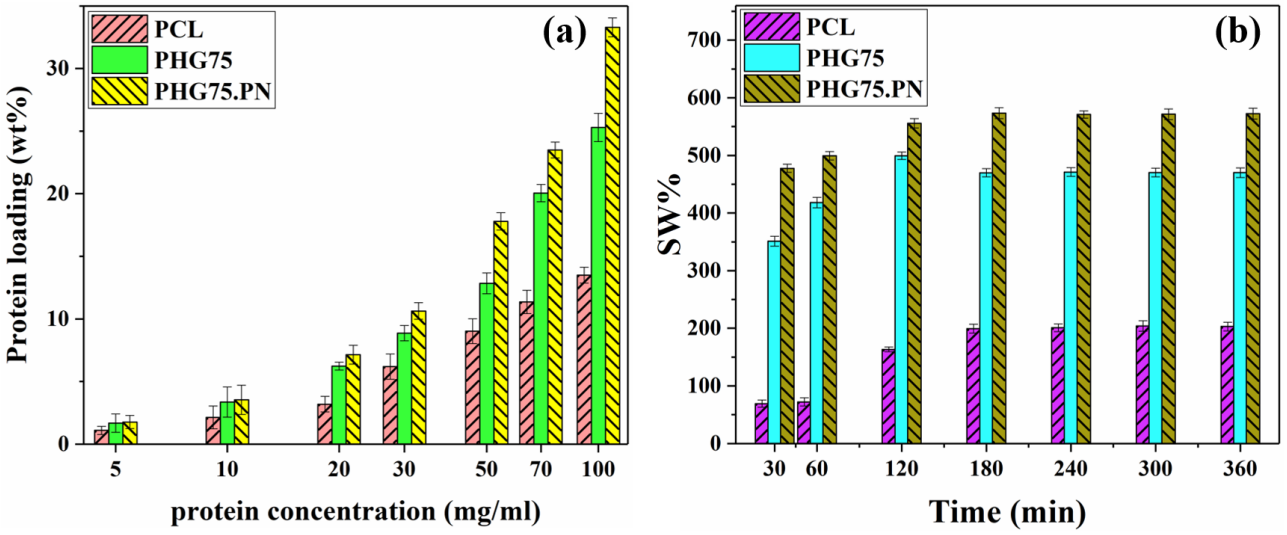

Fig. 6. (a) Effect of support type on the amount of enzyme loading (b) swelling behavior of the PCL, PHG75 nad PHG75.PN.

3.2.3. Catalytic activity of the free and immobilized enzyme in different pH and temperature.

The effect of temperature on the activity of free and immobilized cellulase was investigated over a temperature range of 25-75 °C in an acetate buffer (50mM, pH5.5). The results (Fig. 7a) showed that the optimum temperature for both immobilized and free cellulase was 55 °C. Increase in the temperature to 75 ℃ (for 1 h) led to the decrease in the hydrolytic activity of free and immobilized enzymes to 68% and 78% respectively. This activity reduction can be attributed to the conformational

changes in enzyme structure. As the unique structure of each enzyme is held together by weak forces between the amino acid residues in a polypeptide chain and high temperature leads to break down of these internal interactions resulting a a change in protein conformation including active sites. Therefore, the substrate no longer fits in the active sites and the rate of the reaction is negatively affected. Interestingly, the results (Fig. 7a) illustrated no significant decrease in activity of the enzyme upon immobilization. Even the immobilized enzyme was shown a higher activity at 75℃ demonstrating the reported effect of higher thermal stability due immobilization[8].

The thermal stability of the free and immobilized cellulase was also investigated at 75℃ after 180 min (in acetate buffer 50mM at pH 5.5). As shown in Fig. 7d, the immobilized cellulase could retain 41% of its activity after 180 min, while the free enzyme retained only ~20% of its initial activity. The higher thermal stability of the immobilized enzyme might be due to the ionic interaction between the protein molecules and the hybrid support which offered more rigidity for the enzyme's 3-D structure and has decreased conformational changes at high temperatures. In fact, the assumption was that the given energy to the system at high temperatures at first is consumed to dissociate the interactions between the enzyme and hybrid support instead of denaturing the active sites of the enzyme. The effect of the different support materials on the maintenance of immobilized cellulase activity at high temperatures is shown in Table. S3. As the table shows, the designed hybrid support had the best effect on the tertiary structure of the enzyme, having highest residual activity after 3 h (41%), compared with 10%, 40%, and 35% residual activity for cellulase immobilized on magnetic and silica nanoparticles[40], clay[41] and magnetic nanoparticles at 80 ℃[42].

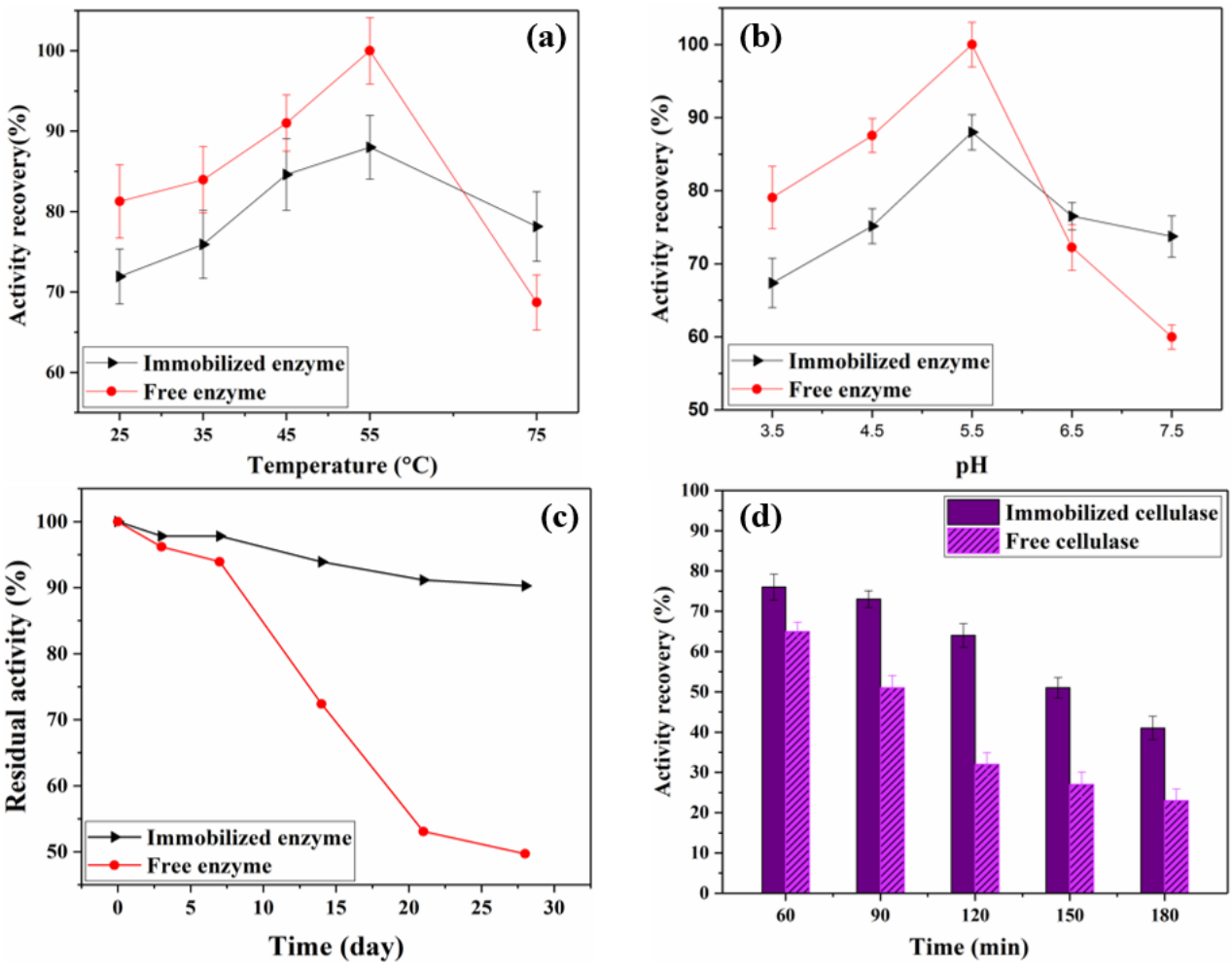

Fig. 7. Effect of (a) temperature and (b) pH on the activity recovery of the free and immobilized enzyme, (c) Storage stability of immobilized and free enzyme at 4 °C for 4 weeks, (d) Thermal stability of the free and immobilized cellulase at 75°C in an acetate buffer 50mM, pH5.5

The effect of pH on the activity recovery of the free and immobilized enzyme was examined within the pH range of 3.5 -7.5. Both free and immobilized enzymes displayed highest activity at pH5.5 (Fig. 7b). In particular, the activity of the immobilized enzyme was higher than those of free enzymes at the alkaline pH. Enzymes are amphoteric molecules containing a large number of amino acids with different charges according to their acid dissociation constants. The total net charge of the enzyme at different pH has a critical effect on the reactivity of the active sites. As the optimal activity pH for the free and immobilized enzymes were similar, it can be confirmed that the immobilization process

caused no changes in the protein structure and the microenvironment of the enzyme. Additionally, the high stability of immobilized enzymes over a wider pH range might be attributed to the buffer function of the hybrid support. In acidic solutions, the hybrid support would contain positive charges caused by the protonated PANI and the cationic hydrogel. Thus, the repulsion force between H^+ ions and positive charges in the hybrid support prevented the absorption of hydrogen ions by the active site and changing the net charge. On the other hand, at the higher pH, the concentration of H^+ in the reaction solution became lower while the charge of the hybrid support was still positive, so the OH^- ions could be absorbed and consumed by the positively charged hybrid support. Therefore, the cellulase stability and activity enhanced in a wide pH range via the protection and buffer function of the prepared hybrid support.

3.2.4. Storage stability of the free and immobilized enzyme

The stability of enzymes during storage is one of the most vital issues because of the high sensitivity of enzymes toward denaturation. The effect of storage time on the activity of the free and immobilized enzyme was determined over a period of 4 weeks (at pH5.5 and 4 °C). Free enzyme lost ~50% of its initial activity after 4 weeks (Fig. 7c), whereas the immobilized enzyme retained 90% of its activity. This could be ascribed to the reduced flexibility of immobilized enzymes due to the formation of ionic interactions between the enzyme and PHG75.PN, which led to a reduced denaturation of the enzyme. Positive effect of immobilization on storage stability of laccase, peroxidase, and cellulase is already reported in literatures [40,43,44].

3.2.5. The kinetic constant of the free and immobilized enzyme

The kinetic parameters including K_m and V_{max} values of the immobilized and free enzyme were calculated with the Lineweaver-Burk plot (Fig. S8) and mentioned in Table 1. As shown in Fig. S8, these values were 2.893 g/l and 7.626 $g.l^{-1}min^{-1}$ for immobilized cellulase and 1.539 g/l and 6.799 $g.l^{-}$

$^{1}min^{-1}$ for free enzyme, respectively. According to Eq.7, when the K_m is equal to the substrate concentration ([S]=K_m), the reaction rate is half of the maximum value (V=V_{max}/2). Therefore, a partial increase in K_m after immobilization indicated the reaction achieved its maximum catalytic efficiency at slightly higher substrate concentrations. It can be attributed to the substrate access restriction to the enzyme active site and/or conformational changes of the enzyme and decreasing the possibility of formation of an enzyme-substrate complex.

The increase in the V_{max} of immobilized cellulase compared to that of the basic enzyme may be due to increased stability of the enzyme after immobilization which reduces its denaturation. Table 1 shows a comparison between thye results of this study and some other studies. As shown in Table 1, the hybrid support developed in this work not only had no significant effect on substrate affinity as Km increased slightly, but also showed a better effect on reaction rate than other nanostructure support materials. Although Km increased from 1.5 to 2.9 mg/ml after immobilization, it was still almost as high as other reports showing the positive effects of the developed hybrid support. More interestingly, the reaction rate (Vmax) in this study was almost 2 times higher than other reports, which is a valuable result for industrial processes.

Table 1. Comparison between kinetic constants of immobilized enzyme in different literature.

Support	V_{max} (g. $l^{-1}min^{-1}$)	K_m (g. l^{-1})	Ref.
Fe3O4@SiO2–graphene oxide composites	5.047	2.31	[45]
Superparamagnetic nanoparticles	0.14	6.51	[46]
magnetic nanocomposite	0.580	3.49	[8]
multiwalled carbon nanotubes	1.7	2.5	[47]
silica nanoparticles	0.565	1.3	[38]
Present study	7.6	2.9	-

3.2.6. Reusability of immobilized enzyme

Although hydrogels have gained considerable attention as a solid matrix for protein immobilization, an inherent drawback of such supports is leaching of the immobilized enzymes, which reduces their reusability. Therefore, a PANI-cationic hydrogel composite nanofiber support was developed to achieve ionic interactions between protonated PANI-cationic hydrogels and the anionic enzyme, in addition to physicochemical interactions (polar and hydrophobic forces) to minimize leaching. A reusability study with 9 catalytic cycles (at 55 °C) using both insoluble (filter paper) and soluble (CMC) substrate was followed (Fig. 8). It was known that the insoluble substrate could only be hydrolyzed by the loose and surface enzymes, while the immobilized enzymes could access the soluble substrate such as CMC. Thus, the use of both soluble and insoluble substrates for recycling highlights the importance of the immobilization of the enzyme on the designed support.

The retain activity of the immobilized enzyme after the 9^{th} hydrolysis cycle of CMC and filter paper was found to be 73.0% and 12.0%, respectively. In general, the gradual loss of activity for both substrates could be related to the denaturation of the enzyme during the different cycles. We assumed that if the immobilized enzyme molecules, when leached, would have access to the insoluble substrate. Therefore, in the case of the insoluble substrate, the enzymatic activity would not decrease significantly in the subsequent cycles.

In our case, high enzymatic hydrolysis was observed in insoluble support (filter paper) in the first three cycles, which then decreased in subsequent cycles. The increasing activity in the first cycles can be attributed to the swelling of the support (Fig. 6b), which allows the loosely bound enzymes to be released. The subsequent decrease in hydrolysis of filter paper shows the decreased release of enzymes as well as the inaccessibility of the insoluble substrate to the active sites. On the other hand, the enzymatic hydrolysis of CMC (soluble support) does not decrease significantly, indicating that it is almost intact over 9 cycles, indicating excellent activity of the immobilized enzyme and its reusability. Comparision of the reusability results in this study with physically adsorbed or entrapped enzymes in

other reports[8,17,45] shows the influence of applied chemical adsorption in addition to entrapment on enzymatic function.

From Fig. S9. it can be seen that the free enzyme has the same activity toward CMC and filter paper, whereas the immobilized enzyme has a lower activity toward filter paper (decrease to 88%) than toward CMC (decrease to 94%), which is due to the intermolecular steric hindrance of the enzyme, blockage of the active site, decrease in the flexibility of the 3D structure of the enzyme, change in the microenvironment of the enzyme, random orientation of the enzyme on the support and so on. However, despite these disadvantages, immobilization would lead to improvement in thermal stability, storability and recyclability, which are crucial in industrial processes. Considering these advantages, it seems that by choosing a suitable support material and immobilization method, we can balance the advantages of activity and immobilization.

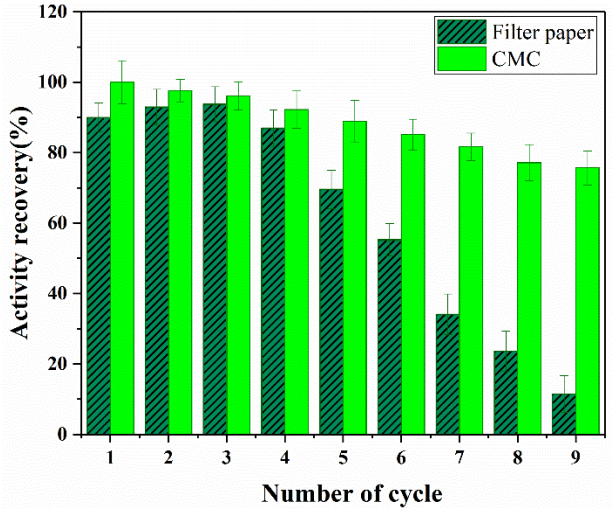

Fig. 8. Reusability of the immobilized enzyme using CMC and Whatman filter paper as the substrate.

4. Conclusion

In summary, a simple two-steps approach was developed to fabricate a conductive nano hydrogel. First, the cationic nano hydrogel was prepared by the electrospinning method with a diameter of around 469 nm followed by template-less PANI nanorods synthesis via in situ polymerization. The formation

of the hybrid matrix was confirmed by FT-IR, FE-SEM, and BET analysis. The hybrid support was used to immobilize the enzyme and immobilization efficiency of up to 96% was achieved just after 1h incubation time owing to the swelling behavior, porosity, and high specific surface area. There was no change in the optimum pH and temperature of immobilized enzyme activity compared to that of the free enzyme. The immobilized enzyme displayed excellent stability at 75°C after 180 min.

The hydrolysis of cellulosic materials with the immobilized enzyme will often have problems of separating the biocatalyst from the final residue of the process. As portability is one of the benefits of nanofibrous matrixes, we used this nanostructure to overcome this drawback. Therefore, we used a newly synthesized cationic hydrogel that showed high adsorption capacity in our previous study and could be prepared in the form of nanofibers in combination with other polymers. In other words, in addition to being a nanostructure, the support texture is like fabric so we can simply take it out and immerse it into another reaction bath without any significant decrease in the enzyme activity. To overcome the blockage of the active site and facilitate the protein to access the substrate, we successfully synthesized highly porous PANI nanorods on the surface of the nanofiber hydrogel without using any templates, contrary to some reports [18, 20-21]. We have eliminated one step and do not need any post-synthesis steps after polymerization. All in all, fabric texture-like of the designed hybrid support leads to having easy-to-use support which can simply separate from the final residue of a process. In addition, due to the good conductivity and biocompatibility of PANI which is reported in some literature, the ability of the prepared support can be investigated as a blood sugar biosensor immobilizing glucose oxidase, urease, etc. Furthermore, the ability of enzyme attachment of support, its biocompatibility, and conductivity makes it a good candidate as a scaffold in tissue engineering.

Notes

Authors declare no conflicting interests.

5. Acknowledgments

The authors would like to express their special appreciation to the Isfahan University of Technology for their financial support.

References

(1) Bilal, M.; Anh Nguyen, T.; Iqbal, H. M. N. Multifunctional Carbon Nanotubes and Their Derived Nano-Constructs for Enzyme Immobilization – A Paradigm Shift in Biocatalyst Design. *Coordination Chemistry Reviews* **2020**, *422*, 213475. https://doi.org/10.1016/j.ccr.2020.213475.

(2) Valikhani, D.; Bolivar, J. M.; Viefhues, M.; McIlroy, D. N.; Vrouwe, E. X.; Nidetzky, B. A Spring in Performance: Silica Nanosprings Boost Enzyme Immobilization in Microfluidic Channels. *ACS Applied Materials & Interfaces* **2017**, *9* (40), 34641–34649. https://doi.org/10.1021/acsami.7b09875.

(3) Morshed, M. N.; Behary, N.; Bouazizi, N.; Guan, J.; Chen, G.; Nierstrasz, V. Surface Modification of Polyester Fabric Using Plasma-Dendrimer for Robust Immobilization of Glucose Oxidase Enzyme. *Scientific Reports* **2019**, *9* (1), 15730. https://doi.org/10.1038/s41598-019-52087-8.

(4) Wang, Y.; Chen, D.; Wang, G.; Zhao, C.; Ma, Y.; Yang, W. Immobilization of Cellulase on Styrene/Maleic Anhydride Copolymer Nanoparticles with Improved Stability against PH Changes. *Chemical Engineering Journal* **2018**, *336*, 152–159. https://doi.org/10.1016/j.cej.2017.11.030.

(5) Jordan, J.; Kumar, C. S. S. R.; Theegala, C. Preparation and Characterization of Cellulase-Bound Magnetite Nanoparticles. *Journal of Molecular Catalysis B: Enzymatic* **2011**, *68* (2), 139–146. https://doi.org/10.1016/j.molcatb.2010.09.010.

(6) Zhai, D.; Liu, B.; Shi, Y.; Pan, L.; Wang, Y.; Li, W.; Zhang, R.; Yu, G. Highly Sensitive Glucose Sensor Based on Pt Nanoparticle/Polyaniline Hydrogel Heterostructures. *ACS Nano* **2013**, *7* (4), 3540–3546. https://doi.org/10.1021/nn400482d.

(7) David, M.; Barsan, M. M.; Brett, C. M. A.; Florescu, M. Improved Glucose Label-Free Biosensor with Layer-by-Layer Architecture and Conducting Polymer Poly(3,4-Ethylenedioxythiophene). *Sensors and Actuators B: Chemical* **2018**, *255*. https://doi.org/10.1016/j.snb.2017.09.149.

(8) Hosseini, S. H. A. H.; Hosseini, S. H. A. H.; Zohreh, N.; Yaghoubi, M.; Pourjavadi, A. Covalent Immobilization of Cellulase Using Magnetic Poly(Ionic Liquid) Support: Improvement of the Enzyme Activity and Stability. *Journal of Agricultural and Food Chemistry* **2018**, *66* (4), 789–798. https://doi.org/10.1021/acs.jafc.7b03922.

(9) Bayramoğlu, G.; Metin, A. Ü.; Arıca, M. Y. Surface Modification of Polyacrylonitrile Film by Anchoring Conductive Polyaniline and Determination of Uricase Adsorption Capacity and Activity. *Applied Surface Science* **2010**, *256* (22). https://doi.org/10.1016/j.apsusc.2010.04.077.

(10) Mubarak, N. M.; Wong, J. R.; Tan, K. W.; Sahu, J. N.; Abdullah, E. C.; Jayakumar, N. S.; Ganesan, P. Immobilization of Cellulase Enzyme on Functionalized Multiwall Carbon Nanotubes. *Journal of Molecular Catalysis B: Enzymatic* **2014**, *107*, 124–131. https://doi.org/10.1016/j.molcatb.2014.06.002.

(11) Labus, K.; Wolanin, K.; Radosiński, Ł. Comparative Study on Enzyme Immobilization Using Natural Hydrogel Matrices—Experimental Studies Supported by Molecular Models Analysis. *Catalysts* **2020**, *10* (5), 489. https://doi.org/10.3390/catal10050489.

(12) Ramirez, M.; Guan, D.; Ugaz, V.; Chen, Z. Intein-Triggered Artificial Protein Hydrogels That Support the Immobilization of Bioactive Proteins. *Journal of the American Chemical Society* **2013**, *135* (14), 5290–5293. https://doi.org/10.1021/ja401075s.

(13) Falcone; Shao; Rashid; Kraatz. Enzyme Entrapment in Amphiphilic Myristyl-Phenylalanine Hydrogels. *Molecules* **2019**, *24* (16). https://doi.org/10.3390/molecules24162884.

(14) Shin, Y. J.; Kameoka, J. Amperometric Cholesterol Biosensor Using Layer-by-Layer Adsorption Technique onto Electrospun Polyaniline Nanofibers. *Journal of Industrial and Engineering Chemistry* **2012**, *18* (1). https://doi.org/10.1016/j.jiec.2011.11.009.

(15) Ince, A.; Bayramoglu, G.; Karagoz, B.; Altintas, B.; Bicak, N.; Arica, M. Y. A Method for Fabrication of Polyaniline Coated Polymer Microspheres and Its Application for Cellulase Immobilization. *Chemical Engineering Journal* **2012**, *189–190*, 404–412. https://doi.org/10.1016/j.cej.2012.02.048.

(16) Trey, S.; Jafarzadeh, S.; Johansson, M. In Situ Polymerization of Polyaniline in Wood Veneers. *ACS Applied Materials & Interfaces* **2012**, *4* (3), 1760–1769. https://doi.org/10.1021/am300010s.

(17) Wu, J. C.-C.; Ray, S.; Gizdavic-Nikolaidis, M.; Uy, B.; Swift, S.; Jin, J.; Cooney, R. P. Nanostructured Bioactive Material Based on Polycaprolactone and Polyaniline Fiber-Scaffolds. *Synthetic metals* **2014**, *198*, 41–50.

(18) Ansari, S. P.; Anis, A. Conducting Polymer Hydrogels. In *Polymeric Gels*; Elsevier, 2018; pp 467–486. https://doi.org/10.1016/B978-0-08-102179-8.00018-1.

(19) Ding, H.; Zhong, M.; Kim, Y. J.; Pholpabu, P.; Balasubramanian, A.; Hui, C. M.; He, H.; Yang, H.; Matyjaszewski, K.; Bettinger, C. J. Biologically Derived Soft Conducting Hydrogels Using Heparin-Doped Polymer Networks. *ACS Nano* **2014**, *8* (5), 4348–4357. https://doi.org/10.1021/nn406019m.

(20) Joseph, N.; Varghese, J.; Sebastian, M. T. Self Assembled Polyaniline Nanofibers with Enhanced Electromagnetic Shielding Properties. *RSC Advances* **2015**, *5* (26), 20459–20466.

(21) Guo, H.; He, W.; Lu, Y.; Zhang, X. Self-Crosslinked Polyaniline Hydrogel Electrodes for Electrochemical Energy Storage. *Carbon* **2015**, *92*, 133–141. https://doi.org/10.1016/j.carbon.2015.03.062.

(22) Khoshnevisan, K.; Vakhshiteh, F.; Barkhi, M.; Baharifar, H.; Poor-Akbar, E.; Zari, N.; Stamatis, H.; Bordbar, A.-K. Immobilization of Cellulase Enzyme onto Magnetic Nanoparticles: Applications and Recent Advances. *Molecular Catalysis* **2017**, *442*, 66–73. https://doi.org/10.1016/j.mcat.2017.09.006.

(23) Andriani, D.; Sunwoo, C.; Ryu, H.-W.; Prasetya, B.; Park, D.-H. Immobilization of Cellulase from Newly Isolated Strain Bacillus Subtilis TD6 Using Calcium Alginate as a Support Material. *Bioprocess and Biosystems Engineering* **2012**, *35* (1–2), 29–33. https://doi.org/10.1007/s00449-011-0630-z.

(24) Nazir, R.; Parida, D.; Guex, A. G.; Rentsch, D.; Zarei, A.; Gooneie, A.; Salmeia, K. A.; Yar, K. M.; Alihosseini, F.; Sadeghpour, A.; Gaan, S. Structurally Tunable PH-Responsive Phosphine Oxide Based Gels by Facile Synthesis Strategy. *ACS Applied Materials & Interfaces* **2020**, *12* (6), 7639–7649. https://doi.org/10.1021/acsami.9b22808.

(25) Parida, D.; Moreau, E.; Nazir, R.; Salmeia, K. A.; Frison, R.; Zhao, R.; Lehner, S.; Jovic, M.; Gaan, S. Smart Hydrogel-Microsphere Embedded Silver Nanoparticle Catalyst with High Activity and Selectivity for the Reduction of 4-Nitrophenol and Azo Dyes. *Journal of Hazardous Materials* **2021**, *416*, 126237. https://doi.org/10.1016/j.jhazmat.2021.126237.

(26) Noonan, K. J. T.; Gillon, B. H.; Cappello, V.; Gates, D. P. Phosphorus-Containing Block Copolymer Templates Can Control the Size and Shape of Gold Nanostructures. *Journal of the American Chemical Society* **2008**, *130* (39), 12876–12877. https://doi.org/10.1021/ja805076y.

(27) Jevremović, A.; Bober, P.; Mičušík, M.; Kuliček, J.; Acharya, U.; Pfleger, J.; Milojević-Rakić, M.; Krajišnik, D.; Trchová, M.; Stejskal, J.; Ćirić-Marjanović, G. Synthesis and Characterization of Polyaniline/BEA Zeolite Composites and Their Application in Nicosulfuron Adsorption. *Microporous and Mesoporous Materials* **2019**, *287*, 234–245. https://doi.org/10.1016/j.micromeso.2019.06.006.

(28) Sheldon, R. A.; van Pelt, S. Enzyme Immobilisation in Biocatalysis: Why, What and How. *Chem. Soc. Rev.* **2013**, *42* (15), 6223–6235. https://doi.org/10.1039/C3CS60075K.

(29) Kruger, N. J. The Bradford Method for Protein Quantitation. In *The protein protocols handbook*; Springer, 2009; pp 17–24.

(30) Ghose, T. K. Measurement of Cellulase Activities. *Pure and Applied Chemistry* **1987**, *59* (2), 257–268.

(31) Green, M.; Allsop, N.; Wakefield, G.; Dobson, P. J.; Hutchison, J. L. Trialkylphosphine Oxide/Amine Stabilised Silver Nanocrystals—the Importance of Steric Factors and Lewis Basicity in Capping Agents. *Journal of Materials Chemistry* **2002**, *12* (9), 2671–2674.

(32) Zhou, W.; Guo, Y.; Zhang, H.; Su, Y.; Liu, M.; Dong, B. A Highly Sensitive Ammonia Sensor Based on Spinous Core–Shell PCL–PANI Fibers. *Journal of Materials Science* **2017**, *52* (11), 6554–6566. https://doi.org/10.1007/s10853-017-0890-3.

(33) Crean (neé Lynam), C.; Lahiff, E.; Gilmartin, N.; Diamond, D.; O'Kennedy, R. Polyaniline Nanofibres as Templates for the Covalent Immobilisation of Biomolecules. *Synthetic Metals* **2011**, *161* (3–4), 285–292. https://doi.org/10.1016/j.synthmet.2010.11.037.

(34) Bade, K.; Tsakova, V.; Schultze, J. W. Nucleation, Growth and Branching of Polyaniline from Microelectrode Experiments. *Electrochimica Acta* **1992**, *37* (12), 2255–2261. https://doi.org/10.1016/0013-4686(92)85120-A.

(35) Shadi, L.; Karimi, M.; Entezami, A. A. Preparation of Electroactive Nanofibers of Star-Shaped Polycaprolactone/Polyaniline Blends. *Colloid and Polymer Science* **2015**, *293* (2), 481–491. https://doi.org/10.1007/s00396-014-3430-6.

(36) Thiemann, C.; Brett, C. M. A. Electrosynthesis and Properties of Conducting Polymers Derived from Aminobenzoic Acids and from Aminobenzoic Acids and Aniline. *Synthetic Metals* **2001**, *123* (1), 1–9. https://doi.org/10.1016/S0379-6779(00)00364-7.

(37) Thommes, M.; Kaneko, K.; Neimark, A. v.; Olivier, J. P.; Rodriguez-Reinoso, F.; Rouquerol, J.; Sing, K. S. W. W. Physisorption of Gases, with Special Reference to the Evaluation of Surface Area and Pore Size Distribution (IUPAC Technical Report). *Pure and Applied Chemistry* **2015**, *87* (9–10), 1051–1069. https://doi.org/10.1515/pac-2014-1117.

(38) Ikeda, Y.; Parashar, A.; Bressler, D. C. Highly Retained Enzymatic Activities of Two Different Cellulases Immobilized on Non-Porous and Porous Silica Particles. *Biotechnology and Bioprocess Engineering* **2014**, *19* (4), 621–628.

(39) Schwarte, L. M.; Podual, K.; Peppas, N. A. Cationic Hydrogels for Controlled Release of Proteins and Other Macromolecules; 1998; pp 56–66. https://doi.org/10.1021/bk-1998-0709.ch003.

(40) Grewal, J.; Ahmad, R.; Khare, S. K. Development of Cellulase-Nanoconjugates with Enhanced Ionic Liquid and Thermal Stability for in Situ Lignocellulose Saccharification. *Bioresource Technology* **2017**, *242*, 236–243. https://doi.org/10.1016/j.biortech.2017.04.007.

(41) Bayramoglu, G.; Senkal, B. F.; Arica, M. Y. Preparation of Clay–Poly(Glycidyl Methacrylate) Composite Support for Immobilization of Cellulase. *Applied Clay Science* **2013**, *85* (1), 88–95. https://doi.org/10.1016/j.clay.2013.09.010.

(42) Abraham, R. E.; Verma, M. L.; Barrow, C. J.; Puri, M. Suitability of Magnetic Nanoparticle Immobilised Cellulases in Enhancing Enzymatic Saccharification of Pretreated Hemp Biomass. *Biotechnology for Biofuels* **2014**, *7* (1). https://doi.org/10.1186/1754-6834-7-90.

(43) Sun, H.; Yang, H.; Huang, W.; Zhang, S. Immobilization of Laccase in a Sponge-like Hydrogel for Enhanced Durability in Enzymatic Degradation of Dye Pollutants. *Journal of Colloid and Interface Science* **2015**, *450*, 353–360. https://doi.org/10.1016/j.jcis.2015.03.037.

(44) Jun, L. Y.; Mubarak, N. M.; Yon, L. S.; Bing, C. H.; Khalid, M.; Jagadish, P.; Abdullah, E. C. Immobilization of Peroxidase on Functionalized MWCNTs-Buckypaper/Polyvinyl Alcohol Nanocomposite Membrane. *Scientific Reports* **2019**, *9* (1), 2215. https://doi.org/10.1038/s41598-019-39621-4.

(45) Li, Y.; Wang, X.-Y.; Jiang, X.-P.; Ye, J.-J.; Zhang, Y.-W.; Zhang, X.-Y. Fabrication of Graphene Oxide Decorated with Fe3O4@SiO2 for Immobilization of Cellulase. *Journal of Nanoparticle Research* **2015**, *17* (1), 8. https://doi.org/10.1007/s11051-014-2826-z.

(46) Xu, J.; Huo, S.; Yuan, Z.; Zhang, Y.; Xu, H.; Guo, Y.; Liang, C.; Zhuang, X. Characterization of Direct Cellulase Immobilization with Superparamagnetic Nanoparticles. *Biocatalysis and Biotransformation* **2011**, *29* (2–3), 71–76. https://doi.org/10.3109/10242422.2011.566326.

(47) Ahmad, R.; Khare, S. K. Immobilization of Aspergillus Niger Cellulase on Multiwall Carbon Nanotubes for Cellulose Hydrolysis. *Bioresource Technology* **2018**, *252*, 72–75. https://doi.org/10.1016/j.biortech.2017.12.082.